NUMERICAL STUDY ON FAST FILLING OF 70 MPA HYDROGEN VEHICLE CYLINDER

ABSTRACT

During the fast filling of hydrogen vehicle cylinder there will be significant temperature rise, and the temperature rise should be controlled under the temperature limit (85 ºC) of the structure material, because it may lead to the failure of the structure. In this paper, a 2-dimionsional axisymmetric computational fluid dynamics (CFD) model for fast filling of 70 MPa hydrogen vehicle cylinder is presented. The numerical simulations are based on the modified standard k - ε turbulence model. Additionally, both the equation of state for hydrogen gas and the thermodynamic properties are calculated by National Institute of Standards and Technology (NIST) datebase: REFPROP 7.0. The thermodynamic responses of fast filling under different pressure-rise patterns and filling times have been explored by the simulation results.

1.0 INTRODUCTION

Hydrogen has been recognized as the primary choice of future secondary energy [1, 2]. And as a kind of fuel, hydrogen is cleaner and more effective than petrol. So it has been widely accepted as the fuel material of fuel cell vehicles (FCV) [3]. For the commercialization of hydrogen FCV, there are many kinds of hydrogen storage technology, such as solid state hydrogen storage, slush hydrogen storage, high pressure gaseous hydrogen storage, etc. Compared with other methods, high pressure gaseous hydrogen storage is more developed and practical. But there are still some problems for high pressure storage method. One of the concerned issues is fast filling of the vehicle cylinder, which also has been discovered in the compressed natural gas vehicle (CNG) [4]. During the filling process of both compressed natural gas (CNG) and hydrogen gas, there is significant temperature rise in the cylinder. And most of high pressure vehicle cylinders are made of carbon fiber reinforced polymer (CFRP), which is temperature-sensitive. Excessive temperature rise may lead to the failure of the carbon fiber, so some standards have restricted that the maximum temperature inside the hydrogen storage cylinder has to be below 85 ºC [5, 6]. The temperature rise may also cause the underfilling of hydrogen gas, which leads to insufficiency of hydrogen filling.

Many investigators have done experiments, simulations and theoretical studies on the issue of the temperature rise during fast filling process. Most of the researches on fast filling concentrate on the cases with the highest working pressure of 35 MPa, such as Monde et al.[7], Liu et al.[8], Dicken and Merida [9, 10], Heitsch et al.[11], Zhao et al.[12], Kim et al.[13], Hiroshi et al.[14] and Toshihiro et al.[15]. But because of the insufficient storage capacity, 35 MPa storage system is hard to meet the demand of 500 km driving range. And 70 MPa hydrogen storage system has become the primary research objective of high pressure hydrogen storage technology.

So far, fast filling experiments of 70 MPa cylinder have been done by Hiroshi et al.[14] and Khan et al.[16], and the theoretical analysis of fast filling process can be found in Yang [17]. For the pressure as high as 70 MPa, the comprehensive understanding of fast filing process is necessary for safety and risk control, which is very hard to achieve only by the experiments. The numerical study is an alternate way for understanding of fast filling process, and today there is still no mathematic model and simulation study on the case with working pressure as high as 70 MPa.

In this paper, a CFD model including modified standard k-ε turbulence and real gas model is presented to predict the fast filling process of 70 MPa, 74 L and type III hydrogen vehicle cylinder. And the thermodynamic responses of fast filling under different pressure-rise patterns and filling times have been explored by the simulation results.

2.0 MATHEMATIC MODEL

2.1 Model Assumptions

According to the real fast filling process, assumptions are proposed for simplifying the model, which are described as follow:

(1) The heat exchange coefficient of convection and the ambient temperature are considered as constant;
(2) The heat transfer characteristic of CFRP is considered as isotropy.
(3) The model is based on 2-dimensional axis symmetry algorithm. The buoyancy effect is neglected.
(4) The temperature of inlet gas is considered as a constant, which is the same as ambient temperature.
(5) The initial temperature of the whole system is considered as the ambient temperature. And the initial pressure is stable at the very beginning of the filling process.

2.2 Model equations

Based on assumptions in Section 2.1, the CFD model is built, in which the heat transfer, turbulence, real gas effects are considered. The governing equations of the flow are described below.

The mass conservation equation:

$$\frac{\partial \rho}{\partial t}+\frac{\partial}{\partial x_i}(\rho u_i)=0 \tag{1}$$

Where ρ is the density, t is the time, u denotes the velocity tensor and x denotes the distance. The subscript i indicates the direction and i = 1, 2, 3 denote x, y, z direction respectively.

In inertial coordinate system, the law of conservation of momentum yields the equations below:

$$\frac{\partial}{\partial t}(\rho u_i)+\frac{\partial}{\partial x_j}(\rho u_i u_j)=-\frac{\partial p}{\partial x_i}+\frac{\partial}{\partial x_j}\left[\mu\left(\frac{\partial u_i}{\partial x_j}+\frac{\partial u_j}{\partial x_i}-\frac{2}{3}\delta_{ij}\frac{\partial u_l}{\partial x_l}\right)\right]+\frac{\partial\left(-\rho\overline{u_i' u'}_j\right)}{\partial x_j} \tag{2}$$

Where p is the pressure and subscript j and l has the same meaning with i. In this model, Reynolds averaging techniques are applied. The superscript ' means the turbulent fluctuating component and superscript - denotes the Reynolds time-averaged component.

A modified standard k - ε model is adopted as the turbulence model. The model [18] is a semi-empirical model based on model transport equations for the turbulence kinetic energy k and its dissipation rate ε. The model transport equation for k is derived from the exact equation, while the model transport equation for ε was obtained using physical reasoning and bears little resemblance to its mathematically exact counterpart.

The turbulence kinetic energy k and its rate of dissipation ε are obtained from the following transport equations:

$$\frac{\partial}{\partial t}(\rho k)+\frac{\partial}{\partial x_i}(\rho k u_i)=\frac{\partial}{\partial x_j}\left[\left(\mu+\frac{\mu_t}{\sigma_k}\right)\frac{\partial k}{\partial x_j}\right]+G_k-\rho\varepsilon-Y_M \tag{3}$$

$$\frac{\partial}{\partial t}(\rho\varepsilon)+\frac{\partial}{\partial x_i}(\rho\varepsilon u_i)=\frac{\partial}{\partial x_j}\left[\left(\mu+\frac{\mu_t}{\sigma_\varepsilon}\right)\frac{\partial\varepsilon}{\partial x_j}\right]+C_{1\varepsilon}G_k\frac{\varepsilon}{k}-C_{2\varepsilon}\rho\frac{\varepsilon^2}{k} \tag{4}$$

In the equations, G_k represents the generation of turbulence kinetic energy due to the mean velocity gradients, calculated as described in eq.(5).

$$G_k=-\rho\overline{u_i'u_j'}\frac{\partial u_j}{\partial x_i} \tag{5}$$

Y_M represents the contribution of the fluctuating dilatation in compressible turbulence to the overall dissipation rate, calculated as described in eq.(6).

$$Y_M=2\rho\varepsilon\mathrm{M}_t^2 \tag{6}$$

Where M_t is the turbulent Mach number, defined as

$$\mathrm{M}_t=\sqrt{\frac{k}{a^2}} \tag{7}$$

Where a is the speed of sound.

The turbulent viscosity μ_t is computed by combining k and ε, defined as follows:

$$\mu_t=\rho C_\mu\frac{k^2}{\varepsilon} \tag{8}$$

$C_{1\varepsilon}$, $C_{2\varepsilon}$,and C_μ are constants ($\mathrm{C}_{1\varepsilon}$= 1.52, $\mathrm{C}_{2\varepsilon}$= 1.92).

As the varying range of the hydrogen properties during the fast filling is quite large, a real gas model must be adopted. The commercial library - NIST Reference Fluid Thermodynamic and Transport Properties (REFPROP) 7.0 includes a series of real gas model, which have a hydrogen model with good accuracy. The modified Benedict-Webb-Rubin equation of state is adopted to calculate the PVT relationship.

The modified Benedict-Webb-Rubin equation of state is described as below, which is expressed as a function of temperature and density.

$$P=\sum_{n=1}^{9}\alpha_n\rho^n+exp\left[\left(\rho/\rho^{crit}\right)^2\right]\sum_{n=10}^{15}\alpha_n\rho^{2n-17} \tag{9}$$

where ρ^{crit} is the critical density, and α_i are functions of temperature resulting in a total of 32 adjustable parameters. And all of the thermodynamic properties can be found in Younglove and Mclinden [19].

2.3 Model validation

This model is validated by the previous 35 MPa experimental data of Liu et al.[8]. For instance, the mass average temperature rise of gas vs. time curve is shown in Fig. 1 for the case, which is initialized with 3 MPa and linear pressure-rise pattern. The simulation results generally agree with the experiment data, and the deviation may mainly caused by the nonlinearity of experiment pressure-rise pattern, and the pattern of simulation is exactly linear.

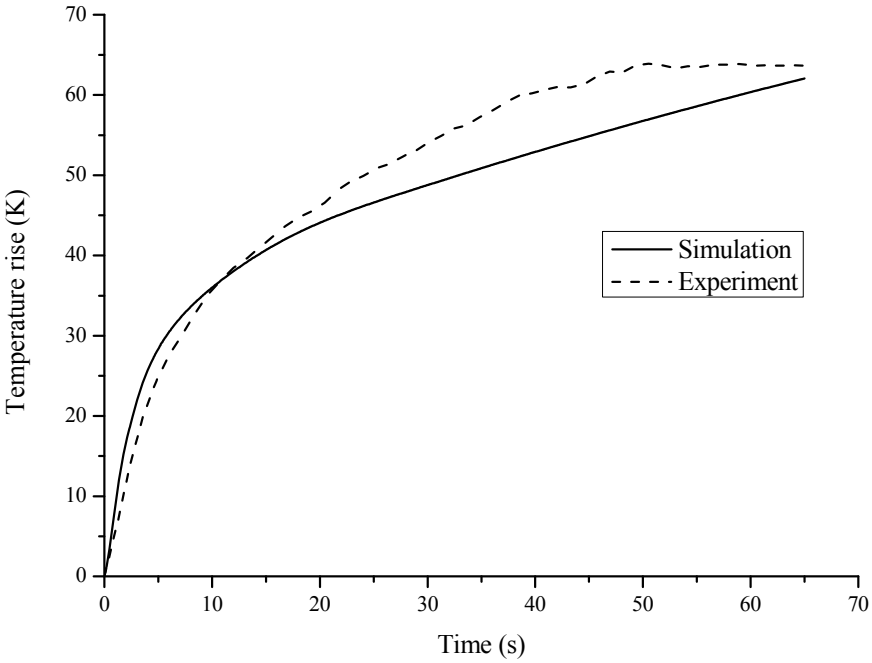

Figure 1. Mass average temperature rise vs. time curve

2.4 Model setup

The volume of the type III cylinder is 74 L, and the structure diagram is shown in Fig. 2. The diameter of inlet pipe is 10 mm. The cylinder is treated as a combination of two parts: fiber layer and aluminum alloy linear.

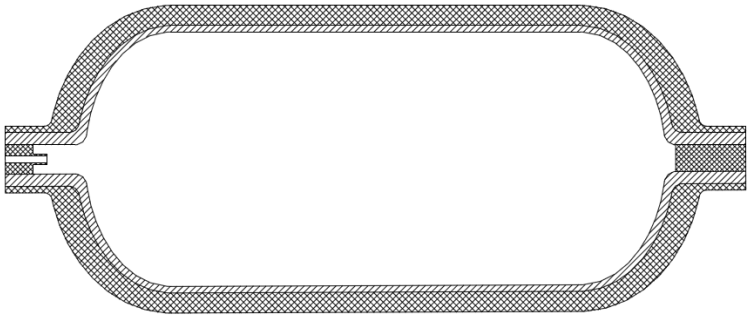
Figure 2. Structure diagram of the 70MPa vehicle cylinder

In all cases, the heat exchange coefficient of convection was assumed as 6 $W/m^2 \cdot K$ for the outer wall of the fiber layer, and the ambient temperature is 278 K. The wall of inlet pipe is assumed as heat insulation. The initial pressure of the hydrogen gas for all cases is 2.0 MPa, and the initial temperature is as the same as the ambient temperature.

The main difference among the previous simulation researches of fast filling is the setting of inlet boundary, which directly dominates the thermodynamic response and the corresponding strategy of the temperature control during the filling process. And there are two kinds of inlet boundary: pressure inlet and constant mass flow rate inlet. The mass flow rate inlet is based on the neglect of variation of inlet flow rate. But during the actual experiment, the control of fast filling is mainly performed by regulating the inner pressure of cylinder, which shows the superiority of pressure inlet boundary.

In this model, the gas inlet is treated as pressure inlet. For different cases, the inlet pressure-rise patterns are set respectively, and the temperature of inlet gas is assumed as the ambient temperature. The inlet pressure-rise patterns for different cases in this paper are shown in Fig. 3.

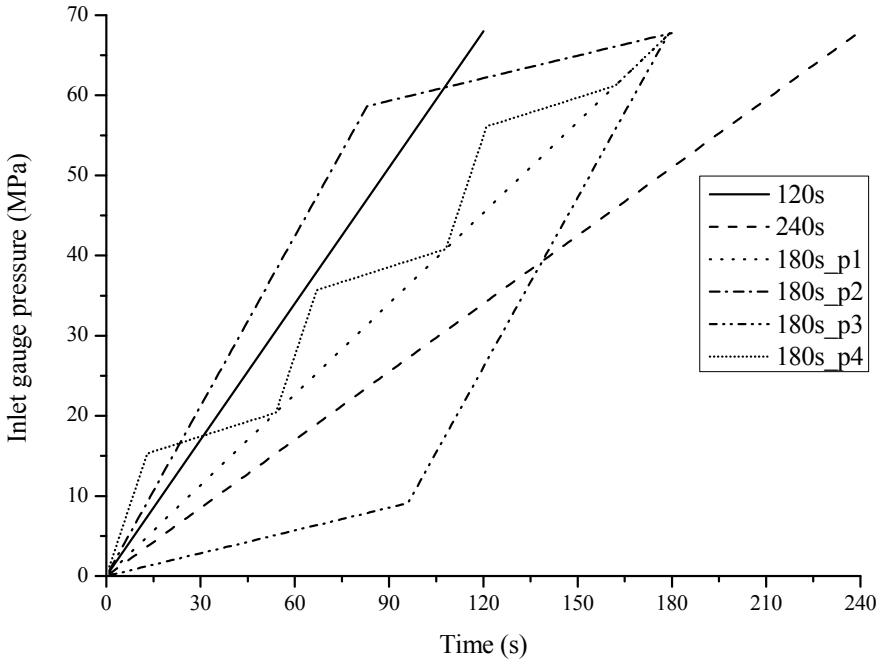

Figure 3. Inlet pressure-rise patterns of different cases

3.0 RESULTS AND DISCUSSION

Fig. 4 shows the temperature contour of the cylinder after 160 seconds for the case of 180s_p1. There is significant temperature gradient between the aluminum alloy linear and the carbon fiber layer. The highest temperature appears in the near-wall space between the inlet jet and the inlet end enclosure. Because the inlet gas temperature is the lowest in the cylinder, there is also significant temperature gradient along the jet path.

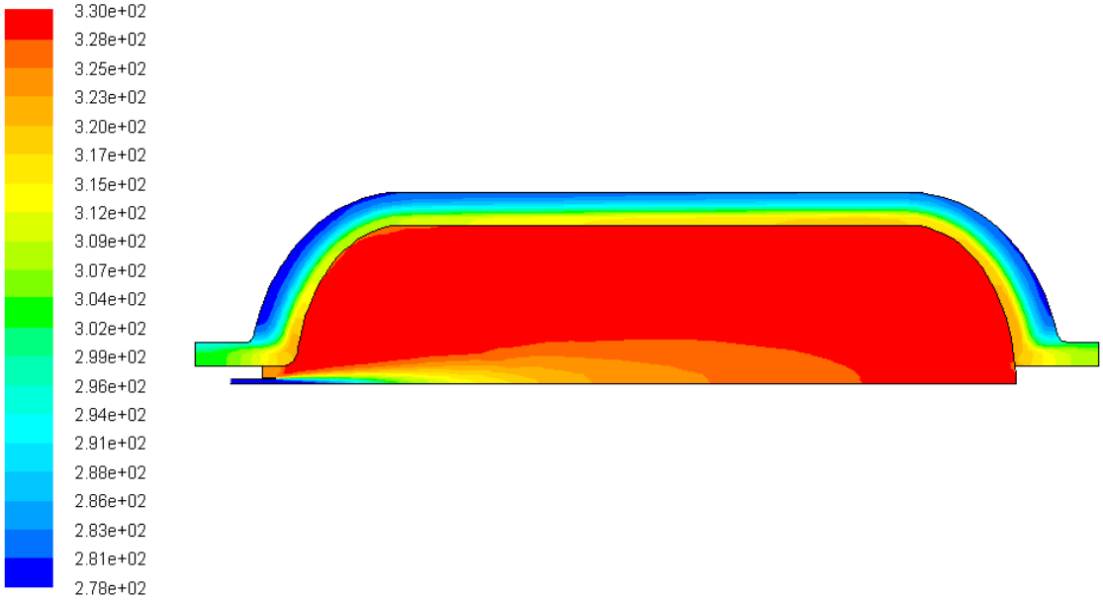

Figure 4. Temperature contour of the cylinder after 160 seconds for the case of 180s_p1

3.1 Effects of filling time

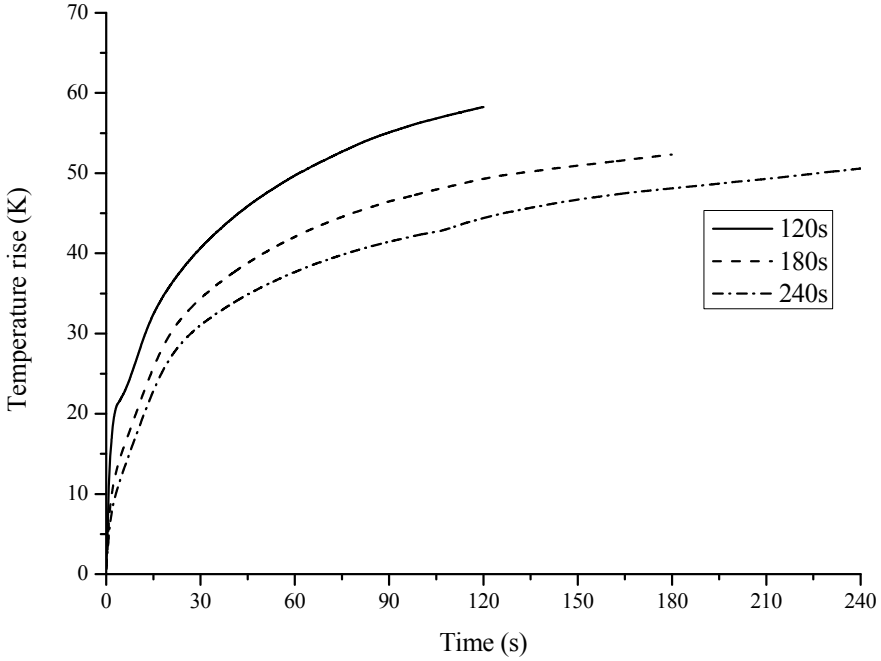

Figure 5. Mass average temperature rise vs. time curve of different filling time

As shown in Fig. 5, the mass average temperature rise vs. time curve of different filling time shows that the total temperature rise decreases with the increasing of filling time. When the pressure-rise rate is higher, there will be much higher temperature rise during the filling. The temperature differences among the results may be mainly caused by the differences of the time derivative of volume average density, which can be equivalent to the inlet mass flow rate. As the transient inlet mass flow rate increases (shown in Fig. 6), the heat which comes from the same period of filling increases too. And the difference among the final temperature rises may be caused by the different performances of heat transfer between hydrogen gas and the cylinder, because the heat can not be transferred to the ambient if the filling time is too short.

Similarly, the inlet mass flow rates also show identical tendency, which is shown in Fig. 6. As the inlet gauge pressure rises, the mass flow rate rises rapidly to a certain limit in the first seconds. Then the rate is falling down with nonlinearity during the residual time, which indicates the nonlinearity change of hydrogen gas density. And the slope of the falling rate increases with the decreasing of the filling time, which indicates the flaw of mass flow inlet boundary. Obviously, the nonlinearity is caused by the real gas effects of hydrogen gas. Additionally, if the filling time is long enough, the inlet is more similar to the constant mass flow rate inlet.

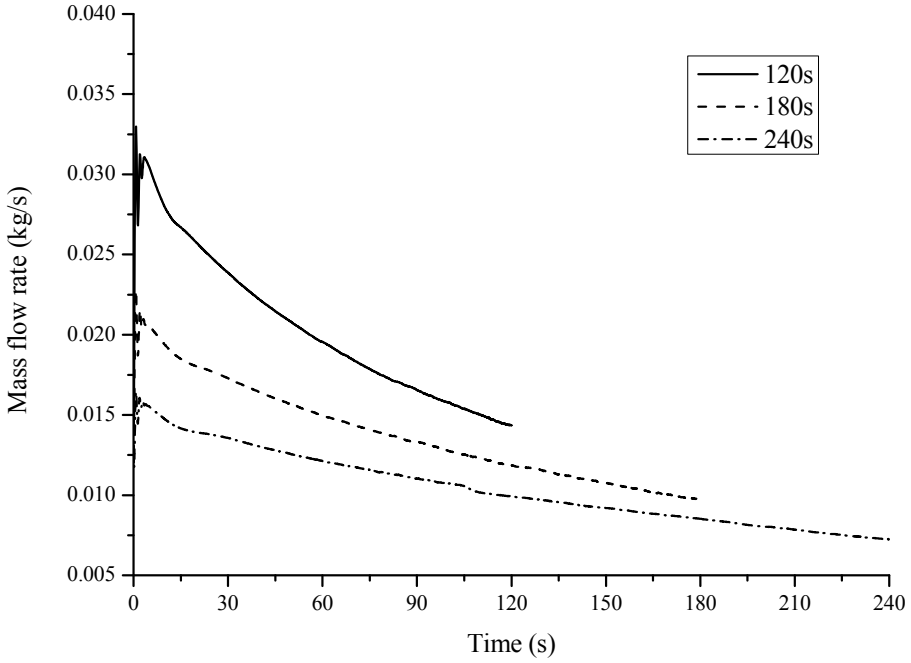

Figure 6. Inlet mass flow rate vs. time curve of different filling time

For the commercialization of FCV, the state of charge (SOC) is also concerned, which is described in eq. (10).

$$SOC = \frac{\rho_{end}}{\rho_0} \tag{10}$$

Where ρ_{end} is the final average density after the filling process in the cylinder. ρ_0 is the density of 288 K and the target pressure, such as 70 MPa in this case.

Fig. 7 shows the variation tendency of SOC during the filling process for different filling time. The final states are 89.7% for 120 s, 90.8% for 180 s and 91.2% for 240 s, and the demand (89%, 180 s) of SAE J 2601 is met. If the filling time is too short, SOC is hard to meet the demand. It means that there is a lower limit time for each filling case.

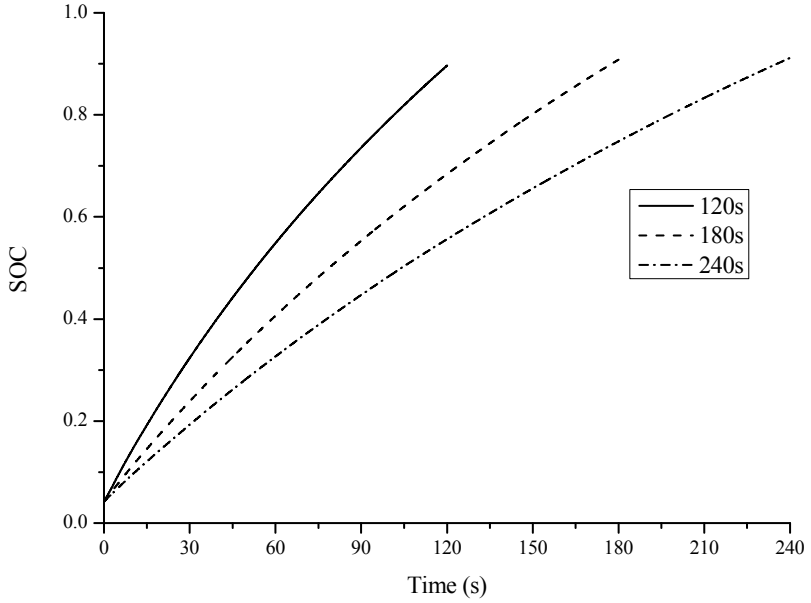

Figure 7. Variation tendency of SOC for different filling time

3.2 Effects of pressure-rise pattern

For the control of temperature rise, the characteristics of different pressure-rise pattern are explored, which are also demonstrated in Fig. 3. In this section, the total filling time is set as 180s.

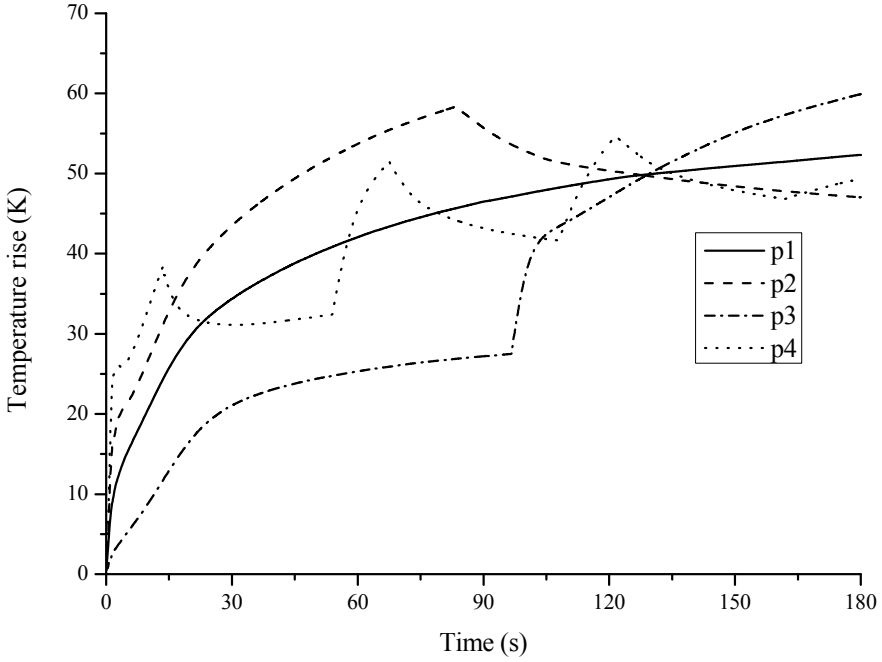

Figure 8. Mass average temperature rise vs. time of different pressure-rise pattern

Fig. 8 shows the mass average temperature rise vs. time curve, which has a similar shape with the experiment result found in Hirotani et al.[14]. The cases with p2 and p3 have a higher maximum temperature rise (approximately 60 K) during the filling process, which may threat the safety of the cylinder with a higher ambient temperature, such as 25 ºC. The differences of final temperature among different pressure-rise patterns may come from the different system cooling efficiency of four cases, especially in the early stage of the filling process.

4.0 CONCLUSIONS

A 2-dimionsional axisymmetric CFD model for predicting fast filling process of 70 MPa hydrogen FCV cylinder has been presented. And by changing the pressure-rise pattern and the filling time, the thermodynamic response of 70 MPa fast filling process has been explored. Some conclusions are described as follows:

(1) For the linear pressure-rise pattern, the mass flow rate rises rapidly to a certain upper limit in the first seconds. Then the rate is falling down with nonlinearity during the residual time. And the gradient of the falling rate increases with the decreasing of the filling time.
(2) If the filling time is too short, SOC is hard to meet the demand of SAE J 2601.

ACKNOWLEDGEMENTS

This research is funded by the key project of national programs for fundamental research and development of China (973 program, Number: 2007CB209706), the high-technology research and development program of China (863 project, Number: 2009AA05Z118), and the Zhejiang Provincial Natural Science Foundation of China (Grant No. Y1100636).

REFERENCES

1. Maus S., Hapke J., Ranong N.C., Wuchner E., Friedlmeier G., Wenger D., Filling procedure for vehicles with compressed hydrogen tanks, *International Journal of Hydrogen Energy*, 33, 2008, pp. 4612-21.
2. Zhang J.S., Fisher T.S., Ramachandran P.V., Gore P.V., Mudawar I., A Review of Heat Transfer Issues in Hydrogen Storage Technologies, *Journal of Heat Transfer*, 127, 2005, pp. 1391-99.
3. McDowall W., Eames M., Forecasts, scenarios, visions, backcasts and roadmaps to the hydrogen economy: A review of the hydrogen futures literature, *Energy Policy*, 34, 2006, pp. 1236-50.
4. Newhouse N.L., Liss W.E., Fast Filling of NGV Fuel Containers, SAE Technical Paper Series 1999-01-3793, SAE (1999).
5. International Standard Organization, Gaseous hydrogen and hydrogen blends - Land Vehicle Fuel Tanks, ISO/DIS 15869.2., 2006.
6. Society of Automotive Engineers, Fueling Protocols for Light Duty Gaseous Hydrogen Surface Vehicles, SAE J 2601-2010.
7. Monde M., Mitsutake Y., Woodfield P.L., and Maruyama S., Characteristics of Heat Transfer and Temperature Rise of Hydrogen during Rapid Hydrogen Filling at High Pressure, *Heat Transfer - Asian Research*, 36, 2007, pp. 13-27.
8. Liu Y.L., Zhao Y.Z., Zhao L., Li X., Chen H.G., Zhang L.F., Zhao H., Sheng R.H., Xie T., Hu D.H., Zheng J.Y., Experimental studies on temperature rise within a hydrogen cylinder during refuelling, *International Journal of Hydrogen Energy*, 35, 2010, pp. 2627-32.
9. Dicken C.J.B., Merida W., Measured effects of filling time and initial mass on the temperature distribution within a hydrogen cylinder during refuelling, *Journal of Power Sources*, 165, 2007, pp. 324-336.
10. Dicken C.J.B., Merida W., Modeling the Transient Temperature Distribution within a Hydrogen Cylinder during Refueling, *Numerical Heat Transfer*, Part A, 53, 2008, pp. 7685-708.
11. Heitsch M., Baraldi D., Moretto P., Numerical investigations on the fast filling of hydrogen tanks, *International Journal of Hydrogen Energy*, 36, 2011, pp. 2606-12.
12. Zhao L., Liu Y.L., Yang J., Zhao Y.Z., Zheng J.Y., Bie H.Y., Liu X.X., Numerical simulation of temperature rise within hydrogen vehicle cylinder during refuelling, *International Journal of Hydrogen Energy*, 35, 2010, pp. 8092-100.
13. Kim S.C., Lee S.H., Yoon K.B., Thermal characteristics during hydrogen fueling process of type IV cylinder, *International Journal of Hydrogen Energy*, 35, 2010, pp. 6830-35.
14. Hiroshi R., Tomioka J., Maeda Y., Mitsuishi H., Watanabe S., Thermal Behavior in Hydrogen Storage Tank for Fuel Cell Vehicle on Fast Filling, In: Proceedings of the 16th World Hydrogen Energy Conference, 13-16 June 2006, Lyon (France).
15. Terada T., Yoshimura H., Tamura Y., Mitsuishi H., Watanabe S., Thermal Behavior in Hydrogen Storage Tank for FCV on Fast Filling (2nd Report), SAE Technical Paper Series 2008-01-0463, SAE (2008).
16. Khan M.T.I., Monde M., Setoguchi T., Hydrogen gas filling into an actual tank at high pressure and optimization of its thermal characteristics, *Journal of Thermal Science*, 18, 2009, pp. 235-240.
17. Yang J.C., A thermodynamic analysis of refueling of a hydrogen tank, *International Journal of Hydrogen Energy*, 34, 2009, pp. 6712-21.

18. El-Gabry L.A., Kaminski D.A., Numerical Investigation of Jet Impingement with Cross Flow-Comparison of Yang-Shih and Standard k - ε Turbulence Models, *Numerical Heat Transfer*, Part A, 47, 2005, pp. 441-469.
19. Younglove B.A., McLinden M.O., An International Standard Equation of State for the Thermodynamic Properties of Refrigerant 123 (2,2‐Dichloro‐1,1,1‐Trifluoroethane), *Journal of Physical and Chemical Reference Data*, 23, 1994, pp. 731-779.